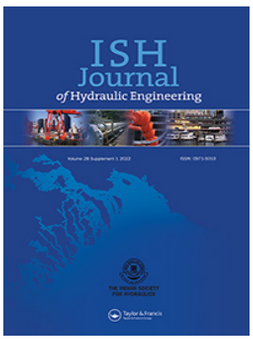

ISH Journal of Hydraulic Engineering

ISSN: (Print) (Online) Journal homepage: https://www.tandfonline.com/loi/tish20

The impulse wheel as hydropower converter for irrigation systems

Gerald Müller, Hannah Williams, Kieran Atkinson, Rory Fleminger, Alexander Goodwin & Natasha Ann Harris

To cite this article: Gerald Müller, Hannah Williams, Kieran Atkinson, Rory Fleminger, Alexander Goodwin & Natasha Ann Harris (2022): The impulse wheel as hydropower converter for irrigation systems, ISH Journal of Hydraulic Engineering, DOI: 10.1080/09715010.2021.2015464

To link to this article: https://doi.org/10.1080/09715010.2021.2015464

Published online: 05 Jan 2022.

ISH JOURNAL OF HYDRAULIC ENGINEERING
https://doi.org/10.1080/09715010.2021.2015464

Taylor & Francis
Taylor & Francis Group

The impulse wheel as hydropower converter for irrigation systems

Gerald Müller[a,b], Hannah Williams[c], Kieran Atkinson[d], Rory Fleminger[d], Alexander Goodwin[d] and Natasha Ann Harris[d]

[a]Faculty of Engineering and Physical Sciences, University of Southampton, Southampton, UK; [b]Soton Hydrodynamics Ltd., Southampton, UK; [c]Faculty of Engineering and Physical Sciences, University of Southampton, Highfield, Southampton, UK; [d]Faculty of Engineering and Physical Sciences, University of Southampton, Southampton, UK

ABSTRACT

There is a significant hydropower potential in irrigation canals worldwide. Much of this potential exists as energy dissipating ramp-type fall structures. Hydropower could be employed to pump water for water saving irrigation, or to generate electricity. This hydropower is unused, since there are no cost-effective hydropower converters for the specific conditions in irrigation canals, i.e. head differences from 0.3 to 5 m and flow volumes ranging from 0.1 to 15 m^3/s. At Southampton University, a simple undershot impulse-type waterwheel with 180° jet deflection was developed specifically for this application. Large scale tests, with a scaling ratio of 1:2.4, showed efficiencies of 53%, confirming predictions from theory. The model employed a novel roller-type power take-off which eliminates the requirement for a cost-intensive gearbox. The impulse wheel has considerable development potential, and could be a cost-effective solution for small hydropower sites at ramp structures.

ARTICLE HISTORY
Received 25 April 2021
Accepted 23 November 2021

KEYWORDS
Micro hydropower; physical model tests; water saving irrigation; renewable energy

1. Introduction

In many irrigation systems, the canals have a shallower gradient than the surrounding land, so that the excess hydraulic power of the water must be dissipated. Typical dissipation structures are ramps with an inclination of 1:1 to 1:3, head differences between 1.5 and 5 m and flow volumes from 0.1 to 15 m^3/s. Ramps are often preferred to vertical drop structures since they allow the energy dissipation in a hydraulic jump rather than in the impact of a vertical jet.

The increasing demand on water resources means that there is a necessity to reduce water usage, which leads to the requirement for water saving irrigation techniques such as drip or sprinkler irrigation systems. There is often also a need to increase the irrigated land area, by pumping water onto fields above canal level, which currently cannot be irrigated. All these applications require power, which is difficult to supply, since grid points are often far away, and diesel pumps can be very expensive. In addition, there is often a necessity to generate electricity in remote rural areas, where settlements are close to irrigation canals. One solution could be, to utilise the existing hydropower in these canals. However, this development of hydropower in irrigation systems is limited by several constraints and boundary conditions:

(1) The head differences range from 0.3 to 5 m, with flow volumes of 0.1 to 15 m^3/s or specific flow volumes of 0.2 to 2.5 $m^3/s/m$.
(2) The hydraulic power ratings range from 0.3 to 750 kW, this is considered as pico, micro and small hydropower.
(3) Farming is often a marginal business, so installations must be cost-effective.
(4) Additional work on, or modifications to the existing infrastructure must be minimal.
(5) In case of a blockage of the Hydropower Converter (HPC), the flow of water must not be impeded.
(6) The HPC must be able to deal with floating material such as branches, reeds etc.
(7) For pumping, the HPC should drive the pumps directly to reduce costs and losses.

Hydropower Converters for application in irrigation systems must be able to function under these conditions.

2. The hydropower resource in irrigation canals

Energy dissipation structures such as ramps, stilling basins and other drop structures are major components of most irrigation systems. Their design is covered in virtually all textbooks on irrigation engineering. Ramps with inclinations of 1:1 to 1:3 are often employed. Information about these energy dissipation structures, or rather the potential hydropower resource in irrigation canals, is however difficult to obtain. The data is mostly held by local authorities, without a centralised database. The authors had access to data for a canal system in Pakistan with a total length of 1120 km and a hydraulic power potential of 79 MW at 1280 sites. Head differences varied between 0.3 and 4.5 m, with flow rates of 0.06 to 67.5 m^3/s and power ratings from 1 kW to 4.5 MW. Figure 1(a) shows the number of drop structures as a function of head difference for all sites, Figure 1(b) the total power as a function of the head difference.

Figure 1 indicates that the majority of the power is contained in the head difference range from 2 to 4.5 m, comprising 279 sites and 55.8 MW. These numbers need to be put into context. The overall power generation capacity in Pakistan including domestic and industrial demand is currently at 0.173 kW per capita. Assuming a conversion efficiency of 70%, the canal could therefore supply 230,000

CONTACT Gerald Müller g.muller@soton.ac.Uk

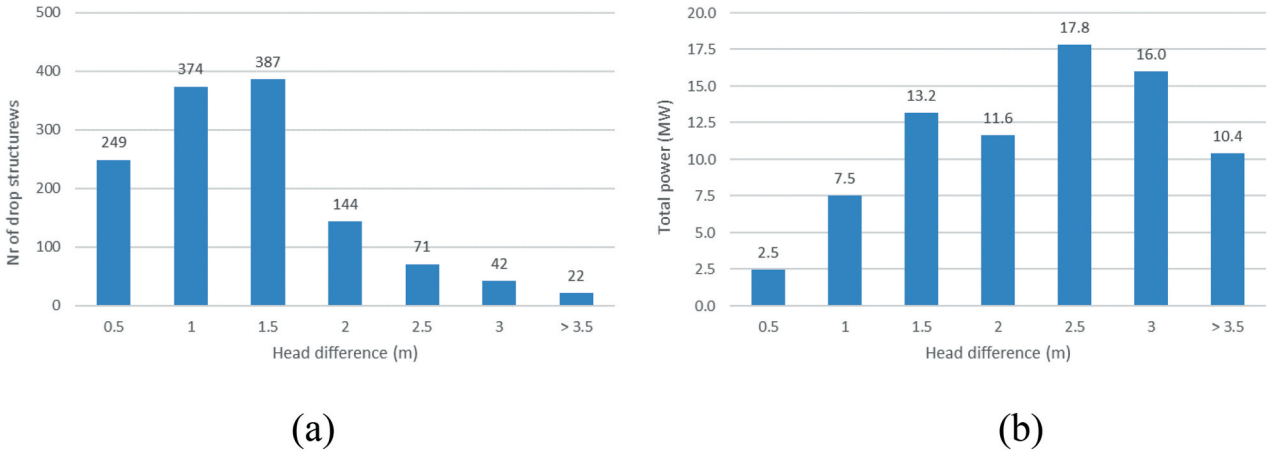

Figure 1. Hydropower potential in the canal system Khyber Paktunkhwar in Peshawar/Pakistan as function of head difference, (a) Number of drop structures, (b) Total power.

Figure 2. Typical small drop structure (Image: Zia Ul-Haq, with permission).

people. or, looking at the pumping capacity, and assuming a pumping demand of 1 litre per second per hectare for an average lift height of 15 m, an additional area of 266 km^2 could be irrigated. Figure 2 shows a typical drop structure, a ramp with a 1:1.5 inclination, a flow volume of 0.9 m^3/s and a head difference of 1.9 m.

The analysis of the available hydropower in irrigation canals in Piedmont, Italy led to similar results, with 44.26% of all sites within a range of 0 to 20 kW, 19.67% for 20 to 40 kW, 14.75% for 46 to 60 kW, 8.2% for 60 to 80 kW and 13.11% for 80 to 100 kW (Butera and Balestra 2015). The majority of sites therefore lies in the range of 1 to 100 kW. Unfortunately, no information on drop heights or drop structure types was given, but economic considerations suggest that the drop heights are in a similar range to the irrigation system analysed above. There is also a strong demand for power in irrigation systems, either to pump water onto fields above canal level, to drive water saving irritation systems, or to generate electricity. The latter application is of particular importance for more remote areas in developing countries. Currently, the utilisation of hydropower in irrigation systems is limited to larger installations with power ratings in the MW range because there are no suitable, cost effective hydropower converters for the typical sites with ultra-low head differences between 2 and 4.5 m, and flow volumes of 0.1 to 15 m^3/s.

3. Requirements and existing technology

The exploitation of hydropower in irrigation canals has been addressed by several researchers. Many of the technologies employed there focus either on the hydrokinetic power of canals, using turbines to generate electricity in fast flowing canals (Niebuhr et al. 2019), or on larger head drops of 6 m to 30 m, where conventional turbine technology can be employed (Jamal and Lewi 2018). One example is the 45-mile hydropower project in Oregon/USA, where there was a 31.6 m existing drop structure with a flow rate of 11 m^3/s in the U.S. Bureau of Reclamation's Main Canal, approximately 45 miles north of the diversion of water into the canal from the Deschutes River in Bend, Oregon. In 2015, three Kaplan turbines of 1.15 MW capacity each were installed to generate hydropower at the site, Hadjerioua et al. (2016).

Most of the potential is however available at much lower head differences. Comparatively little work has however been reported on the potential at lower drop structures, and the development of suitable HPC technology for this scenario. An overview of ultra-low head HPC technology is given in (Boshinova et al. 2013), an overview of the available hydropower technologies in the context of utilisation in irrigation canals in (Loots et al. 2015). The installation of hydropower technology into existing irrigation canals leads to the specific demands listed above. These requirements exclude turbine solutions, where costs of the HPC and the required modifications to the existing canal would be high.

Overshot waterwheels could be a solution for head differences between 2 and 4.5 m. Their efficiencies can reach 85%, and debris can pass through unhindered. However, their flow volume is limited to around 0.2 m^3/s per meter width, so that they are only of interest for very specific conditions with higher head differences and lower flow rates.

In the 19th Century, several types of waterwheels were developed for head differences of 0.5 to 2.5 m and flow rates of up to 6 m^3/s, most notably the *Zuppinger* and

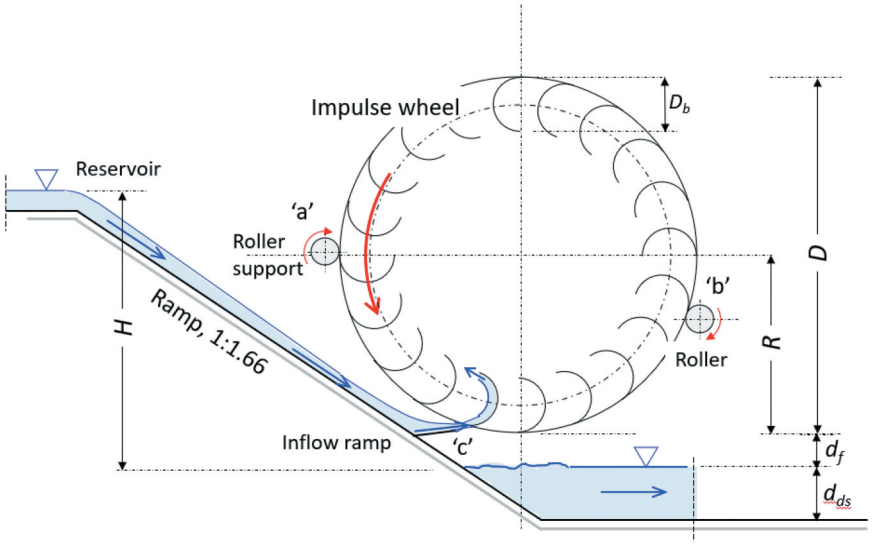

Figure 3. Impulse wheel.

Sagebien wheels (Quaranta and Muller 2018). These wheels have efficiencies of up to 82%, but they require a weir type inflow detail which in the case of a ramp in an irrigation canal, would make a large inflow structure and a bypass channel necessary. The large diameters of these wheels of 7 to 9 m increases costs further. The Archimedes Screw Turbine (AST), an Archimedes screw working in reverse as a hydropower converter, has recently gained popularity due to its simplicity, the high efficiency of more than 80% at full load and their cost advantages, YoosefDoost and Lubitz (2020). AST installations in irrigation canals would however require a bypass channel and control elements, which increases the costs considerably.

Impulse or stream wheels, where the kinetic energy of the flow is employed to generate mechanical power, have been employed since antiquity. Their efficiency is however limited to a theoretical maximum of 29.4% (Quaranta 2018). Such wheels were employed for fast flowing currents. The *Poncelet* wheel was developed by a French hydraulic engineer in the early 19th Century. It had curved blades, where a supercritical jet, which entered the wheel at the bottom, was deflected upwards. The efficiencies were reported to reach 60% (Bozhinova et al. 2013). The supercritical flow was created by a regulated undershot weir, the deflection angle was around 90 degrees. A third type of kinetic energy converter is the *Pelton* turbine, with efficiencies of up to 90%. *Pelton* turbines are employed as pico-HPCs with head differences of 20 m and more. In *Pelton* turbines, the water jet is deflected by nearly 180 degrees, which increases the efficiency. In addition, more than one blade is in contact with the jet. *Pelton* wheels are not suitable for the head differences normally encountered in irrigation canals, but a modification of such a turbine with the aim to adapt the functional principle to lower head differences and flow velocities is possible and will be described in the next section.

Cross flow turbines are impulse type HPCs for head differences between a minimum of 2.5 to 5.0 m (depending on manufacturer) and a maximum of 200 m, with efficiencies up to 85%, e.g. Zhou and Deng (2017). They are relatively simple machines, but still require an active control element which increases complexity and costs. Typical sites in irrigation canals are at or below the minimum head requirements for cross flow turbines, so that their application may not be suitable. In addition, they do not allow the passage of sediment and will require a trash rack to capture larger pieces of floating debris which would not pass through the turbine.

4. The undershot impulse wheel with 180 degree jet deflection

4.1. Overview

At Southampton University, there is an ongoing research programme to develop hydropower solutions for ultra-low head differences, and for application in irrigation systems. Within this project, the undershot impulse wheel was developed as a potential solution for drop structures with head differences of 1.8 to 5 m and flow volumes of 0.2 to 1.5 m^3/s per meter width (Atkinson et al. 2020).

The specific situation at ramps, with head differences of around 2 to 5 m and supercritical flow with velocities of 6 to 9.5 m/s, thicknesses of 50 to 200 mm and jet widths from 0.5 to 4 or even 5 m, requires a specific solution. The existence of the fast jet implies that a kinetic energy converter could be employed. The impulse wheel developed for this purpose is shown in Figure 3.

It has a diameter 'D', with in this case 20 semi-circular buckets of diameter 'D_b'. It is located downstream of the ramp, with a clearance d_f between the bottom of the wheel and the water surface downstream. The inflow ramp at point 'c' is also located at a height of approximately d_f above the downstream water level. The head difference H is taken as the vertical distance between the reservoir water level and the centreline of the jet. The inflow ramp diverts the fast jet of water from the concrete ramp into the wheel. The inflow ramp is adjustable, so that in case of a wheel jam it can be lowered, and the water flows again in its original path below the wheel. No bypass channel is therefore required. Floating debris and gravel can pass through the gap between the inflow ramp and wheel. The wheel can be installed without any interference with, or extension of the existing canal structure. Compared with e.g. turbines, the impulse wheel HPC is quite a simple machine, implying cost-effectiveness.

To increase the efficiency of the impulse wheel, a curved blade was developed which creates a deflection angle of nearly 180 degrees upwards.

One of the major cost items for any waterwheel installation is the gearbox because of the comparatively low speed of the wheel, between 3 and 15 rpm, the resulting need for a high transmission ratio, the high torque and the long life-span of 20 years. The gearbox for a 15 kW waterwheel project amounts to 35 to 40% of the total costs of the installation. (pers. comm.). This wheel does not have a central shaft, but two rollers at points 'a' and 'b' as supports, whereby the downstream roller at 'b' is used for power take-off (PTO). This increases the PTO speed and reduces the torque, thereby reducing costs for gearing considerably (Quaranta et al. 2018)

4.2. Theory

The vertical deflection of the water jet reduces its velocity, this needs to be considered. Figure 4(a) shows the jet deflection. Neglecting friction, since the ramp is short, the initial jet velocity v_0 at the ramp is given by

$$v_0 = \sqrt{2gH} \tag{1}$$

The blade moves with a velocity v_b, the relative velocity v_1 then becomes

$v_1 = v_0 - v_b$(2)

As the jet of thickness t curves upwards, it is deflected by 180 degrees, but it also loses velocity. The relative Total Energy Line (TEL) $TEL_1 = t + {v_1}^2/2\,g$ is reduced by a vertical distance $D_b - t$, and the exit velocity v_2 becomes

$$v_2 = \sqrt{2g(TEL_1 - D_b + t)} \tag{3}$$

The total force on the blade F_b can be determined with the average velocity v_{av}:

$$v_{av} = \frac{v_1 + v_2}{2} \tag{4}$$

In momentum theory, the force F_B created by a horizontal jet of water with a thickness t, and a blade width B which is diverted by an angle γ of more than 90 degrees becomes

$$F_B = 2\rho B t v_{av}^2 (1 + \sin(\gamma - 90)) \tag{5}$$

Power equals force times velocity, the power P then becomes:

$$P = F_B v_b = 2\rho t v_{av}^2 v_b \tag{6}$$

The available kinetic power P_{kin} is

$$P_{kin} = \rho Q \frac{v_0^2}{2} \tag{7}$$

The efficiency η can now be calculated as $\eta = P/P_{kin}$. Figure 4 (b) shows the theoretical efficiency curves for blade diameter and wheel diameter ratios of D_b/D = 0.075, 0.137 and 0.20 with a ratio of d_f/D = 0.05. Interestingly, whilst for small ratios of D_b/D the point of maximum efficiency is near vb/v_0 = 0.33, this point shifts towards vb/v_0 = 0.31 for D_b/D = 0.2. This is caused by the fact that for the same blade velocity v_b, the force on the blade reduces with increasing ratio D_b/D as a function of the square root of the effective blade diameter $D_b - t$, see Eq.(3). The kink in the efficiency curves for $D_b/D > 0.075$ is caused by the fact that from a certain blade velocity onwards, the jet does not have sufficient energy for a complete deflection.

The support on rollers creates a situation where the power generated by the wheel has to be transmitted to the rollers via friction (Quaranta et al. 2018). This is possible since:

(a)Water wheels have a high weight-to-power ratio in the range of 3 to 10 kN per kW, and

(b)through adequate choice of the roller positions, a contact force high enough can exist to ensure that the power can be transferred by friction.

For a wheel with friction PTO two load cases exist. Figure 5(a) shows the load case LC1, dead load only. The force vector diagram shows that the contact forces are larger than the weight of the wheel.

Figure 5(b) shows LC2, operational load. The deflection of the water jet causes a force F_B on the blade assumed to act horizontally at the centre of the blade, and at a distance $R = D_B/2$ away from the wheel centre. At the contact point of roller 'b' with the wheel rim, a friction force F_{fr} transmits the power whereby $F_{fr} = F_B\,R/(R - D_B/2)$. F_B needs to be determined for the situation with the maximum power. The forces for LC2 can be determined analytically as follows.

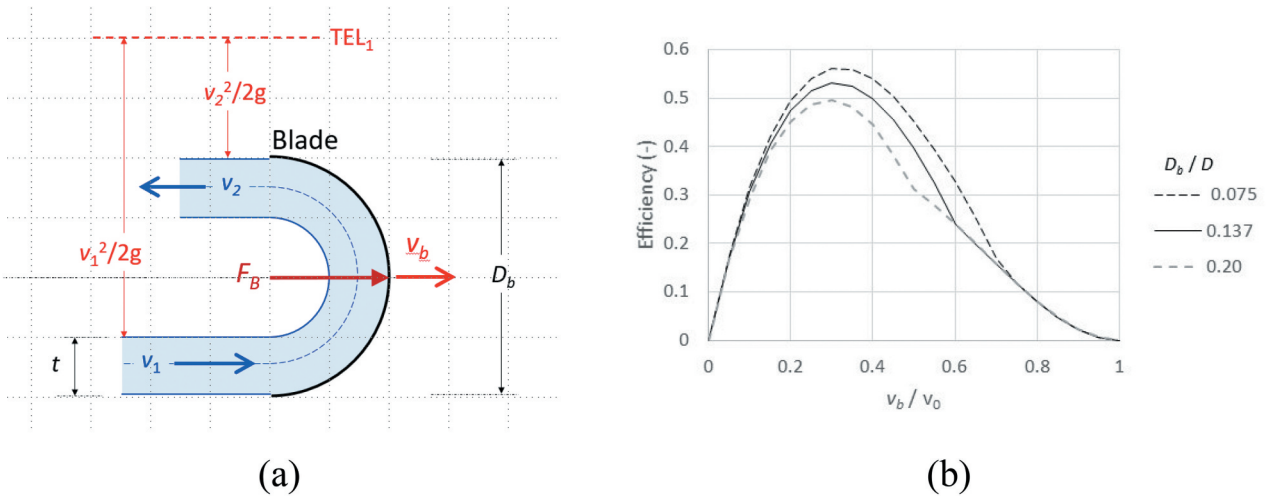

Figure 4. Theory, (a) Jet deflection model, and (b) Efficiency as function of normalised blade velocity.

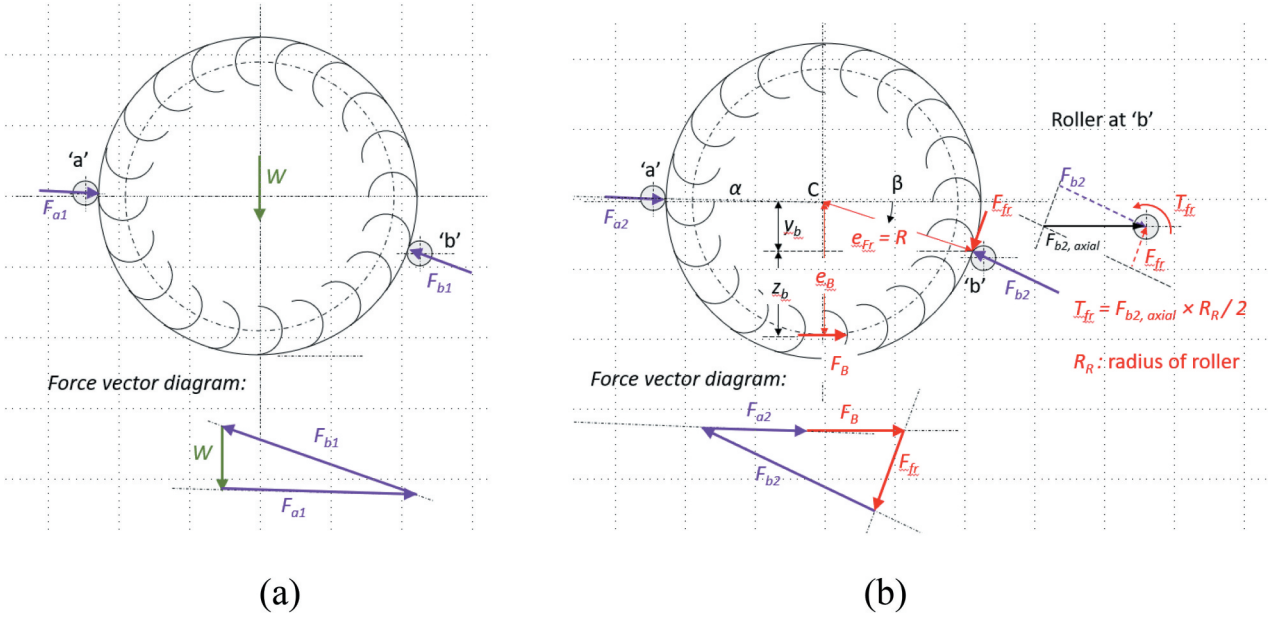

Figure 5. Support reactions, (a) Load case LC1, self weight, (b) load case LC2, hydrodynamic load and power take-off.

Point 'a' The contact points 'a' and 'b' between rollers and the rim of the wheel have known coordinates (x_a, y_a) and (x_b, y_b). The connection with the centre C has angles α and β with the horizontal.

$\alpha = asn\ (y_a/R)$

$\beta = asn\ (y_b/R)(8)$

The unknown forces are the support reactions F_{a2} and F_{b2}.

The lever arm z_{a2} between the line of action of F_{a2} and 'b' is

$z_{a2} = R\ sin\ (\beta - \alpha)(9)$

Taking moments over point ,b', clockwise moments are positive:

$F_{a2} \times z_{a2} - F_B \times (R - D/2 - y_b) = 0(10)$

where F_{a2} is the unknown. This can be resolved for F_{a2}.

The y-component of the support reaction F_{b2} can now be determined from vertical equilibrium:

$F_{b2y} = F_{a2} \times \sin \alpha + F_{fr} \times cos\ \beta$,

and $F_{b2} = F_{b2y}/cos\ \beta(11)$

The friction factor of steel on steel in wet conditions is approximately 0.3. The actual friction force F_{fr} then needs to be equal to, or less than 0.3 ($F_{b1} + F_{b2}$). Figure 5(b) indicates, that the combination of LC1 and LC2 leads to a higher contact force, and thereby a higher friction force which can be transmitted, at point 'b'. This roller should be chosen for the PTO. The axial load on the roller then becomes the vector sum of friction and support load as shown in the detail in Figure 5(b), with an additional torque T_{fr} acting on the roller shaft.

5. Experiments

5.1. Experimental set-up

To assess the hydrodynamic theory as well as the validity of the PTO, physical model tests were conducted. A typical ramp structure, Figure 2, with a head difference of 2 m was chosen as the reference site. The physical model experiments were conducted within a section of a 1.4 m wide and 8 m long tank in the Hydraulics Laboratory at the University of Southampton. The test area had a footprint of approximately 1.4 m × 4.5 m, with an 800 mm deep sump tank at one end, where water could be stored. The flume bottom was checked with a spirit level at both ends of the footprint and found to be horizontal. It was therefore used as a reference plane to determine the vertical distances shown in Figure 6(a). The horizontal distances were

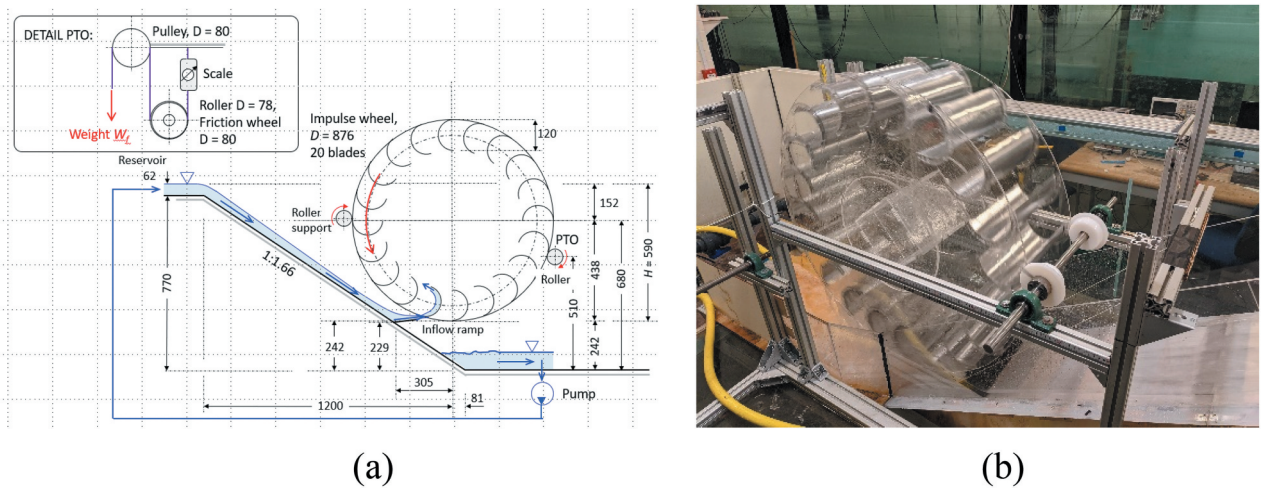

Figure 6. Experiments (a) side elevation of model with dimensions, (b) Side view (image by H Williams).

measured using the position of the wheel centre as reference point. The head difference H was determined from the reference plane and a scale fixed in the reservoir. The flow volume was determined by closing off the exit port of the reservoir, and measuring the time required to increase the water level by 100 mm. The water level was measured with a pointer gauge. This was repeated at the end of the experiment to ensure that the pumping volume had not changed. The maximum flow volume was initially estimated as 10 l/s. The scale was then chosen as 1:2.4 to match the dimensions of the experimental space. The wheel had a diameter of 876 mm, a width of 270 mm, and a weight of 153 N, Figure 6(a).

It was built using two Perspex side disks with 10 mm thickness, the semi-circular blades had a diameter of 120 mm, and were made from 2 mm aluminium sheet.

Using two submersible pumps in the sump, the water was pumped up to the 1.2 m long, 0.5 m wide and 0.4 m deep rectangular reservoir as indicated in Figure 6(a). The water then flowed through a 500 mm wide outlet with a curved wing wall a central guide wall, to minimize hydraulic losses, into a 250 mm wide and 1050 mm long horizontal channel, and then onto the spillway. The spillway itself was constructed using laser cut Perspex of 12 mm thickness, with a plywood base and a gradient of 34°. Figure 6(b) shows the wheel model and the test site. An inflow ramp was incorporated on the slope of the spillway. It consisted of a flat steel plate with a hinge allowing the spillway to be positioned at the optimum angle to direct water into the wheel.

5.2. Power transfer to roller

The model dimensions were chosen so that the roller support could be integrated. The wheel was supported by four 78 mm diameter nylon rollers located at point 'a' at a distance of 20 mm above the centre line, and at point 'b' at 170 mm below the centre line. The weight of the wheel was 153 N, a vector analysis with $\alpha = asn\ (20/438) = 2.6°$ and $\beta = asn\ (170/438) = 22.8°$ gave support reactions of $F_{a1} = 386.8$ N, and $F_{b1} = 424.6$ N. The maximum theoretical power of $P = 30.4$ W was determined using an efficiency of 52.5%, a flow volume of $Q = 0.010$ m^3/s and a total head difference of $H = 0.59$ m.

With a blade speed of 1.11 m/s, corresponding to $v_b = v_0/3$, the blade force F_B for the maximum theoretical power of 30.4 W becomes $F_B = 30.4/1.11 = 27.4$ N. The friction force at the roller was then determined as $F_{fr} = 27.4 \times (438–120/2)/438 = 23.6$ N. Using Eq. (8) to (11), the reaction forces for LC2 can be determined as $F_{a2} = 37.6$ N, and $F_{b2} = 60.5$ N. This results in a total reaction force at 'b' of 424.6 + 60.5 = 485.1 N. With a friction coefficient of 0.1 for Nylon on Perspex, the friction force that can be transmitted is 48.5 N, which is larger than the actual force of $F_{fr} = 23.6$ N. The power transfer with friction is therefore possible. In the experiment, no slippage between roller and wheel could be observed, confirming the analysis.

5.3. Power take-off (PTO)

A Prony-brake was used as power take-off as shown in the detail PTO in Figure 6(a). It consisted of a friction wheel of 80 mm diameter, a pulley, a scale and an applied weight W_f. The scale was fixed to a horizontal support beam. A friction rope was led around the friction wheel and run over a pulley, where a weight W_f was applied. The difference between scale reading and weight constitutes the friction force. The speed of the wheel was measured by timing five revolutions with a stopwatch. The tangential velocity of the friction wheel was multiplied with the friction force to obtain the power P_{out}.

5.4. Experimental results

Two series of tests were conducted, with flow rates of $Q_1 = 0.0086$ m^3/s and $Q_2 = 0.0090$ m^3/s. Figure 7(a) shows the power as function of speed for the tests and from theory, Figure 7(b) the efficiency as function of the normalised speed ratio.

Due to the restrictions in pumping volume, the maximum flow rate achievable was $Q_2 = 0.0090$ m^3/s and the maximum velocity ratio max v_b/v_0 was 0.34. Theory indicates that the maximum efficiency was reached for $v_b/v_0 = 0.31$, so that the measurements just covered that point. The experimental efficiency was determined as the ratio of power out P_{out}, determined from the Prony brake measurements and the speed of the wheel, and the available hydraulic power P_{hyd} for the given head difference H and the flow rate Q. Here, the available hydraulic power is used instead of the kinetic power

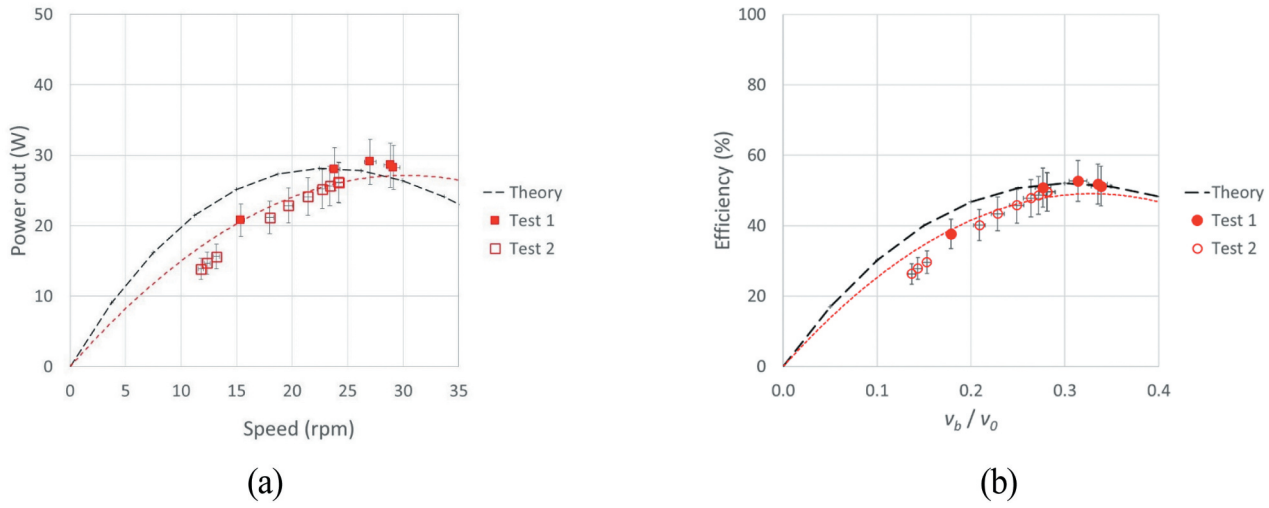

Figure 7. Test results, (a) Power as function of speed, (b) Efficiency as function of velocity ratio.

as determined from Eq. (4) since it includes all hydraulic losses occurring during the transformation of potential to kinetic power as the water flows down from the ramp.

$$\eta = \frac{P_{out}}{\rho g H Q} \tag{12}$$

The experimental results showed a maximum efficiency of 52.7% for $v_b/v_0 = 0.31$, which agrees well with the theoretical value of 53.2%.

An error analysis was conducted, the results are shown as error bars in Figure 5. The principal errors come from the geometry/measurements, volume flow measurement, timing and scale reading of the Prony brake. This resulted in maximum errors of 2% for speed measurements, and 11% for the efficiency values. One parameter which could not be measured is the jet velocity v_0, this was determined from theory. The theory however assumes zero losses, so that the results of the analysis can be considered as conservative.

6. Discussion

6.1. Overview

Large scale tests were conducted to assess the functionality of the roller-type power take-off, ad to determine the power output and efficiency for comparison with theory. The PTO worked reasonably well, and the experimental efficiency agreed well with the theoretical predictions. The limitations of the tests did unfortunately not allow for a more detailed parameter study.

6.2. Blade geometry

The introduction of a 180 degree curved blade resulted in an increased efficiency of 52.7% compared with the 29.4% of a simple stream wheel. The semi-circular blade is however not the optimum geometry for the blade. The effective inflow vector of the jet is the vector sum of the jet, and the tangential velocity vector of the wheel. Observations of the inflow showed that during the contact of the blade with the water jet, the jet was partially deflected downwards and away from the blade, Figure 8(a). This is expected to reduce the power generated by the wheel, since the jet cannot follow the full curvature of the blade. It will connect with the blade at a point inside of the semi- circle which reduces the effective momentum exchange angle. The dashed portion of the inflow jet in Figure 8(a) illustrates this affect. In addition, at the point of contact of jet and blade the inflowing water jet has a radial velocity component which will not contribute to the momentum exchange.

The blade tangent at the inflow point should be parallel to the effective inflow vector, as shown in Figure 8(b), so that these losses cannot are minimised.

The theory of the Pelton wheel implies that more than one blade can be in contact with the water jet, thereby increasing the efficiency of the HPC (Becker 1986). Figure 9 illustrates the concept:

The analysis of the experimental results, and the comparison with Taking the distance between two blades as length l, the initial contact time t_0 is

$$t_0 = \frac{l}{v_0} \tag{13}$$

The blade at point '1′ cuts into the water jet, which has a velocity v_0. When this happens, a short section of length l_j of the water jet is cut off, but remains in contact with blade 2 for a contact time t_1

$$t_1 = \frac{l_j}{v_0 - v_b} \tag{14}$$

The total time Δt a blade is in contact with the water jet is

$$\Delta t = t_0 + t_1 \tag{15}$$

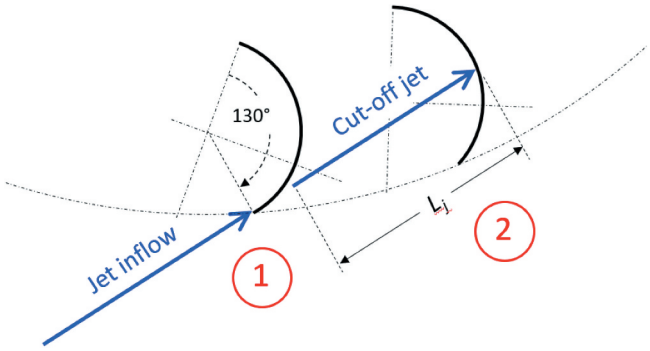

Figure 9. Blades in contact with the water jet.

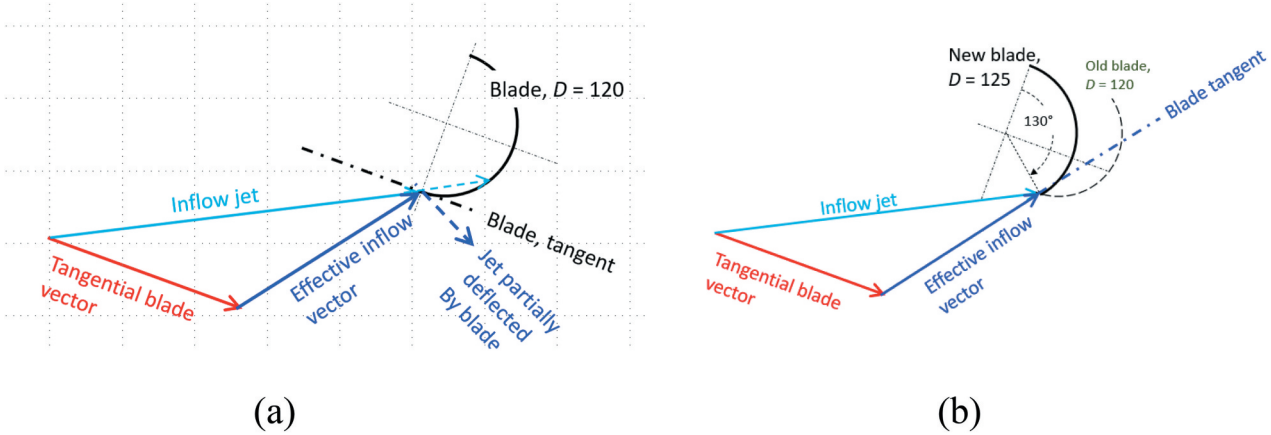

Figure 8. Effective inflow vector (a) Semi-circular blade geometry, (b) Optimised blade shape.

And the effective number of blades n in contact with the water jet becomes

$$n = \frac{\Delta t}{t_0} = \frac{v_0}{v_0 - v_b} \tag{16}$$

This is the average of the number of blades in contact with the water jet at any one time. For the model tests, n becomes

$$n = \frac{3.40}{3.4 - 1.11} = 1.485 \tag{16}$$

This means, that the theoretically possible efficiency is the maximum efficiency of 53.2% multiplied with 1.485, or 78.7%. The situation for the existing blade geometry showed however that this effect in the tests described previously is small since (a) a part of the jet is deflected away from the blade at contact, and (b) the water jet does not enter the blade parallel to the blade tip, see the discussion in the previous section. The use of the simple theory with only one blade, i.e. $n = 1.0$, is therefore justified in this case. In order to achieve this condition for the geometry of the experimental wheel, the blade radius needs to be increased slightly, and that the jet deflection has to be reduced to 130 degrees.

Small scale tests conducted in Southampton with a wheel model of 190 mm diameter and an optimised blade geometry showed efficiencies up to 67% at the design flow rate. The reduction of losses combined with the increase in effective blade number more than outweighed the reduction of F_B due to the reduced angle for momentum exchange (Atkinson et al. 2020).

The theoretical considerations led to several improvements which need to be made:

(1) The blade geometry and number of blades must be optimised.
(2) The inflow ramp must be designed to avoid sideways spilling of water.

6.3. Constant speed operation

Electricity generation from kinetic energy converters usually requires a variable speed operation, since the velocity of the water flow changes with flow volume and the blade speed ratio must be maintained at the point of optimum efficiency. This imposes additional constraints and costs on the system, especially if the electricity needs to be fed into the grid, since the voltage and frequency of the is a function of the wheel speed. If either or both need to be constant, then a frequency inverter is required. The impulse wheel on ramps has the distinct advantage that the inflow velocity is dominated by the drop height, and not by the flow volume, so that the velocity of the inflow jet is constant and the wheel can operate at a constant speed irrespective of the flow rate of the water.

6.4. Scaling

The large scale of the experiments implies that hydraulic scale effects are small. The transmission of power through friction depends on the power-to-weight ratio of the water wheels. From the literature (Müller 1899), the power-to-weight ratio of an overshot waterwheel – which is considered as similar in construction to the impulse wheel described here – could be estimated as 4.5 to 5.5 kN/kW. With a weight of 0.153 kN, and a nominal power output of 50 W (this could not be achieved because of the limited pumping capacity), the model wheel had a power-to-weight ratio of 5 kN/kW. For a geometric scale factor n, power scales with $m^{3.5}$ and weight with m^3, so that the ratio for the model reduces to 3.6 kN/kW. Still, this can be considered as a realistic value. However, the friction factor between wheel and rollers was significantly smaller than the factor expected in reality. In the next test series, a metal outer rim of the wheel and metal rollers should be employed to achieve a realistic modelling of the power take-off.

6.5. Application example

The data can now be employed to assess the site shown in Figure 2, which has a flow rate of 0.9 m^3/s, and a head difference of 1.95 m. Assuming a freeboard $d_f = 0.05$ m, the wheel could generate a mechanical power of 8.9 kW. With a generator efficiency of 0.85, the electricity generated is 7.6 kW. Assuming further a capacity factor of 0.6, this power would be sufficient to supply approximately 24 houses. Alternatively, the power could be used to pump 23 litres per second for a vertical height of 30 m during the irrigation season.

7. Conclusions

A theory for impulse wheels with 180 degree jet deflections with a friction power take-off was developed, and large scale model tests conducted to assess the potential of such wheels for hydropower generation at ramp-type energy dissipators in irrigation canals. It was found that:

- There is a considerable hydropower potential with head differences between 2 and 5 m and power ratings from 0.3 to 750 kW in irrigation canals.
- The theory of an impulse wheel with 180 degree jet deflection suggests maximum efficiencies of up to 53%.
- The power can be transmitted through friction onto rollers with a significantly smaller diameter than the wheel. This reduces PTO costs considerably.
- Experimental efficiencies reached 52.7% for a blade to flow velocity ratio of 0.31, the power transmission through friction was possible.
- The experimental results agreed well with theoretical predictions.
- Further theoretical considerations and small scale model tests showed that here is considerable space for optimisation.

The results shows that the undershot impulse wheel on a roller support works as predicted, has an acceptable efficiency, further development potential and could be a cost-effective solution for the exploitation of ultra-low head hydropower in irrigation canals.

Acknowledgments

The authors would like to acknowledge the financial support from the British Council (Grant Nr 523230522, "*Small, ultra-low head hydropower in irrigation canals*") and the support from Prof. Zia Ul-Haq from the University of Engineering and Technology Peshawar/Pakistan.

Disclosure statement

No potential conflict of interest was reported by the author(s).

Funding

This work was supported by the British Council [523230522].

List of symbols

D:	Diameter of wheel (m)
D_b:	Diameter of blade
d_f:	Freeboard below wheel (m)
e_B:	Distance between line of action of blade force with centre line of wheel
F_a:	Reaction force at point 'a'
F_b:	Reaction force at point 'b'
F_B:	Jet induced force on blade (N)
F_{fr}:	Friction force at point 'b'
H:	Head difference (m)
L_j:	Length of cut-off jet (m)
m:	Scaling factor (-)
n:	Average number of blades in contact with the water jet
P_{out}:	Measured output power (W)
P_{hyd}:	Available hydraulic power (W)
P_{kin}:	Kinetic power (W)
Q:	Flow volume (m^3/s)
R:	Radius of wheel (m)
R_R:	Radius of roller (m)
t:	Thickness of water jet (m)
t_0:	Initial contact time of water jet (seconds)
t_1:	Contact time of cut-off jet (seconds)
T_R:	Torque on roller (Nm)
v:	Velocity (m/s)
v_b:	Blade velocity at centre of blade (m/s)
v_0:	Velocity of water jet at contact with the blade (m/s)
W:	Weight of wheel (N)
W_f:	Weight applied to friction brake (N)
$x_{a,\,b}$:	x-distances from centre C of points 'a' and 'b'
$y_{a,\,b}$:	y-distances from centre C of points 'a' and 'b'
α:	Centre angle of point 'a' with the horizontal (degrees)
β:	Centre angle of point 'b' with the horizontal (degrees)
γ:	Angle of jet deflection (degrees)
ρ:	Density of water (kg/m^3).

References

Atkinson, K., Fleminger, R., Goodwin, A., Harris, N., Paterson, R., and Pearce, N. (2020). *Peshawar hydropower: capturing the hydropower potential from low-head drops within irrigation Canals in Peshawar, Pakistan*, GDP Report. University of Southampton, Faculty of Engineering and Physical Sciences.

Becker, E. (1986). "*Technische Strömungslehre*." Teubner Studienbücher Mathematik, B.G Teubner, Stuttgart, Germany.

Bozhinova, S., Hecht, V., Kisliakov, D., Müller, G., and Schneider, S. (2013). "Hydropower converters with head differences below 2· 5 m." *Proc. Inst. Civ. Eng.: Energy*, 166(3), 107–119. doi:10.1680/ener.11.00037

Butera, I., and Balestra, R. (2015). "Estimation of the hydropower potential of irrigation networks." *Renew. Sust. Energ. Rev.*, 48, 140–151. doi:10.1016/j.rser.2015.03.046

Hadjerioua, B., Christian, M., Lee, K., and Mauer, E. (2016). "Small hydropower development on irrigation canals in the United States: the 45-mile hydropower project 3MW project performance and lessons learned-full story." *HydroVision International Conference*, Minneapolis, USA.

Jamal, J., and Lewi, L. (2018). "Utilization of irrigation flow for the construction of micro-hydro power plant." *AIP Conf. Proc.*, 1977(1), 060018. AIP Publishing LLC.

Loots, I., Van Dijk, M., Barta, B., Vuuren, V., and Bhagwan, S.J. (2015). "A review of low head hydropower technologies and applications in a South African context." *Renew. Sust. Energ. Rev.*, 50, 1254–1268. doi:10.1016/j.rser.2015.05.064

Müller, W. (1899). "*Die eisernen Wasserräder, Berechnung, Konstruktion u. Wirkungsgrad. Teil 1: Die Zellenräder*." Veith & Co, Leipzig, Germany.

Niebuhr, C.M., van Dijk, M., Neary, V.S., and Bhagwan, J.N. (2019). "A review of hydrokinetic turbines and enhancement techniques for canal installations: technology, applicability and potential." *Renew. Sust. Energ. Rev.*, 113, 109240. doi:10.1016/j.rser.2019.06.047

Quaranta, E., Franco, W., Muller, G., and Butera, I. (2018). "Preliminary investigation of an innovative power transmission for low speed water wheels" *5th IAHR Europe Conf.*, Trento/Italy.

Quaranta, E., and Müller, G. (2018). "Sagebien and Zuppinger water wheels for very low head hydropower applications." *J. Hydraul. Res.*, 56(4), 526–536. doi:10.1080/00221686.2017.1397556

Quaranta, E. (2018). "Stream water wheels as renewable energy supply in flowing water: theoretical considerations, performance assessment and design recommendations." *Energy Sustain. Dev.*, 45, 96–109. doi:10.1016/j.esd.2018.05.002

YoosefDoost, A., and Lubitz, W.D. (2020). "Archimedes screw turbines: a sustainable development solution for green and renewable energy generation—a review of potential and design procedures." *Sustainability*, 12(18), 7352. doi:10.3390/su12187352

Zhou, D., and Deng, Z.D. (2017). "Ultra-low-head hydroelectric technology: a review." *Renew. Sust. Energ. Rev.*, 78, 23–30. doi:10.1016/j.rser.2017.04.086